Clinical Cancer Research

Guadecitabine Plus Ipilimumab in Unresectable Melanoma: The NIBIT-M4 Clinical Trial

Anna Maria Di Giacomo[1], Alessia Covre[1], Francesca Finotello[2], Dietmar Rieder[2], Riccardo Danielli[1], Luca Sigalotti[3], Diana Giannarelli[4], Florent Petitprez[5,6,7,8], Laetitia Lacroix[5,6,7], Monica Valente[1], Ornella Cutaia[1], Carolina Fazio[1], Giovanni Amato[1], Andrea Lazzeri[1], Santa Monterisi[1], Clelia Miracco[9], Sandra Coral[1], Andrea Anichini[10], Christoph Bock[11,12,13], Amelie Nemc[11], Aram Oganesian[14], James Lowder[14], Mohammad Azab[14], Wolf H. Fridman[5,6,7], Catherine Sautès-Fridman[5,6,7], Zlatko Trajanoski[2], and Michele Maio[1]

Abstract

Purpose: The immunomodulatory activity of DNA hypomethylating agents (DHAs) suggests they may improve the effectiveness of cancer immunotherapies. The phase Ib NIBIT-M4 trial tested this hypothesis using the next-generation DHA guadecitabine combined with ipilimumab.

Patients and Methods: Patients with unresectable stage III/IV melanoma received escalating doses of guadecitabine 30, 45, or 60 mg/m^2/day subcutaneously on days 1 to 5 every 3 weeks, and ipilimumab 3 mg/kg intravenously on day 1 every 3 weeks, starting 1 week after guadecitabine, for four cycles. Primary endpoints were safety, tolerability, and MTD of treatment; secondary were immune-related (ir) disease control rate (DCR) and objective response rate (ORR); and exploratory were changes in methylome, transcriptome, and immune contextures in sequential tumor biopsies, and pharmacokinetics.

Results: Nineteen patients were treated; 84% had grade 3/4 adverse events, and neither dose-limiting toxicities per protocol nor overlapping toxicities were observed. Ir-DCR and ir-ORR were 42% and 26%, respectively. Median CpG site methylation of tumor samples ($n = 8$) at week 4 (74.5%) and week 12 (75.5%) was significantly ($P < 0.05$) lower than at baseline (80.3%), with a median of 2,454 (week 4) and 4,131 (week 12) differentially expressed genes. Among the 136 pathways significantly ($P < 0.05$; Z score >2 or <−2) modulated by treatment, the most frequently activated were immune-related. Tumor immune contexture analysis ($n = 11$) demonstrated upregulation of HLA class I on melanoma cells, an increase in CD8$^+$, PD-1$^+$ T cells and in CD20$^+$ B cells in posttreatment tumor cores.

Conclusions: Treatment of guadecitabine combined with ipilimumab is safe and tolerable in advanced melanoma and has promising immunomodulatory and antitumor activity.

Introduction

Epigenetic events occurring during cancer development and progression can impair tumor immunogenicity and functional host's T-cell recognition of neoplastic cells, significantly contributing to tumor cell evasion by immune surveillance (1). However, the reversible nature of epigenetic features suggests that epigenetic drugs could be efficiently utilized to potentiate tumor immune recognition. Providing experimental support for this theory, epigenetic immune remodeling of cancer cells by DNA hypomethylating agents (DHAs) was found to improve their immunogenicity and immune recognition via upregulation or induction of molecules of the antigen processing and presentation machinery (1). Among these, a crucial role was identified for HLA class I and accessory/costimulatory molecules, tumor-associated antigens, transporter associated with antigen processing 1/2, and chaperone molecules (2). These phenotypic changes induced or upregulated antigen-specific T-cell recognition of neoplastic

[1]Center for Immuno-Oncology, University Hospital of Siena, Siena, Italy. [2]Biocenter, Division of Bioinformatics, Medical University of Innsbruck, Innsbruck, Austria. [3]Oncogenetics and Functional Oncogenomics Unit, Centro di Riferimento Oncologico di Aviano (CRO) IRCCS, Aviano, Italy. [4]Regina Elena National Cancer Institute, IRCCS, Rome, Italy. [5]INSERM, UMR_S 1138, Centre de Recherche des Cordeliers, Team Cancer, Immune Control and Escape, Paris, France. [6]University Paris Descartes Paris 5, Sorbonne Paris Cite, UMR_S 1138, Centre de Recherche des Cordeliers, Paris, France. [7]Sorbonne University, UMR_S 1138, Centre de Recherche des Cordeliers, Paris, France. [8]Programme Cartes d'Identitié des Tumeurs, Ligue Nationale Contre le Cancer, Paris, France. [9]Pathology Unit, Department of Medical, Surgical and Neurological Science, University of Siena, S. Maria alle Scotte Hospital, Siena, Italy. [10]HumanTumors Immunobiology Unit, Fondazione IRCCS Istituto Nazionale dei Tumori, Milan, Italy. [11]CeMM Research Center for Molecular Medicine of the Austrian Academy of Sciences, Vienna, Austria. [12]Department of Laboratory Medicine, Medical University of Vienna, Vienna, Austria. [13]Max Planck Institute for Informatics, Saarbrücken, Germany. [14]Astex Pharmaceuticals Inc., Pleasanton, California.

Note: Supplementary data for this article are available at Clinical Cancer Research Online (http://clincancerres.aacrjournals.org/).

A.M. Di Giacomo and A. Covre contributed equally to this article.

Corresponding Author: Michele Maio, Center for Immuno-Oncology Medical Oncology and Immunotherapy, Department of Oncology, University Hospital of Siena Viale Mario Bracci, 16 Siena 53100 Italy. Phone: +39 0577 586336; Fax: +39 0577 586303; E-mail: mmaiocro@gmail.com

Clin Cancer Res 2019;25:7351–62

doi: 10.1158/1078-0432.CCR-19-1335

Translational Relevance

Preclinical studies identified a broad immunomodulatory activity of DNA hypomethylating agents (DHAs) in neoplastic cells from solid and hemopoietic malignancies, suggesting their promising role to improve the clinical effectiveness of cancer immunotherapies. This notion, and the unique functional role of cytotoxic T-lymphocyte–associated protein 4 molecule in T-cell activation and expansion, prompted us to explore the clinical relevance of the next-generation DHA guadecitabine combined with ipilimumab. In the proof-of-principle, phase Ib, NIBIT-M4 trial, patients with metastatic melanoma received escalating doses of guadecitabine combined with standard ipilimumab administration. Treatment was feasible, safe, and tolerable, had promising tumor immunomodulatory activity, and showed evidence of clinical activity in melanoma. The initial findings of the NIBIT-M4 trial suggest that DHA-based immunocombination strategies are worth to be further explored in the clinic to improve the efficacy of cancer immunotherapy.

cells (3–5). More recently, DHAs have also been shown to contribute to the activation of cellular immunity by modulating Thelper 1-type (Th1) chemokines (6) and IFN-related genes (7, 8). In addition, the DHA decitabine was also found to enhance $CD8^+$ T-cell activation and proliferation, and to improve the cytolytic activity of human IFN gamma$^+$ T cells, which correlated with improved antitumor responses and survival of patients with solid tumors (9). Of note, decitabine was also demonstrated to revert exhaustion-associated *de novo* methylation programs of CD8 T cells, enhancing their ability to expand in the course of antiprogrammed cell death protein 1 (PD-1) therapy (10). Altogether, these findings supported the use of DHA as suitable agents to improve the clinical effectiveness of cancer immunotherapies (1).

Among clinically available immunotherapeutic agents, the anticytotoxic T-lymphocyte–associated protein 4 (CTLA-4) mAb ipilimumab first provided evidence of therapeutic effectiveness in patients with metastatic melanoma (11); despite the limited number of objective responses observed across a spectrum of doses and schedules in treatment-naïve and pretreated populations, about 20% of patients had long-term survival (12). Recently, improved overall survival (OS) as compared with ipilimumab has been reported in metastatic melanoma using targeting of PD-1 (13). CTLA-4 and PD-1 molecules operate at different stages of T-cell activation: CTLA-4 on naïve T cells typically in the lymph nodes, PD-1 on antigen-experienced T cells, primarily in peripheral tissues (14). Blockade of both molecules favors the expansion of tumor-infiltrating CD8 T cells; however, at variance with PD-1 blockade, CTLA-4 targeting induces a robust CD4 effector T-cell response via the expansion of an $ICOS^+$ Th1-like CD4 subset, thus sustaining long-term antitumor immune responses (14, 15). Despite the higher clinical efficacy of anti–PD-1 monotherapy in metastatic melanoma (13, 16), these findings highlight the unique functional role of the CTLA-4 molecule and support its further clinical exploration. In addition, poor clinical outcome of anti–CTLA-4-treated (but not anti–PD-1-treated) patients with metastatic melanoma was recently found to be associated with downregulation or loss of HLA class I molecules expression by melanoma cells (17).

This comprehensive scenario led us to hypothesize that priming the tumor with DHAs might complement the specific functional role of CTLA-4 molecule and improve the therapeutic efficacy of CTLA-4 blockade in patients with metastatic melanoma. Providing preclinical evidence for this theory, the DHA decitabine (18) or guadecitabine (19) combined with CTLA-4 blockade significantly reduced tumor growth of poorly immunogenic syngeneic grafts compared with single-agent therapy.

Here, we report the safety and biological and clinical activity of a novel DHA-based immunocombination strategy explored in the NIBIT-M4 clinical trial, a phase Ib, dose-escalation study of guadecitabine, combined with ipilimumab in patients with metastatic melanoma. The next-generation DHA guadecitabine was chosen for its higher resistance to degradation by cytidine deaminase, resulting in an *in vivo* prolonged activity (20), compared with its active metabolite decitabine.

Patients and Methods

Study design and participants

The Italian Network for Tumor Biotherapy (NIBIT) Foundation undertook the NIBIT-M4 phase Ib, dose-escalation, single-center study between October 2015 and August 2018 at the Center for Immuno-Oncology of Siena, Italy. The study design is shown in Fig. 1. Adult patients with unresectable stage III or IV cutaneous melanoma, measurable lesions by CT or MRI per WHO criteria that were amenable to biopsy, life expectancy $\geq$16 weeks, Eastern Cooperative Oncology Group performance status $\leq$1, and who had received no more than one line of therapy for advanced disease were eligible for inclusion. Patients were excluded if they had received prior ipilimumab, or if they had primary ocular melanoma, autoimmune disease, or symptomatic brain disease requiring immediate local intervention. The study was conducted in accordance with the ethical principles of the Declaration of Helsinki and the International Conference on Harmonization of Good Clinical Practice. The protocol was approved by the independent ethics committee of the University Hospital of Siena (Siena, Italy). All participating patients (or their legal representatives) provided signed-informed consent before enrolment. The trial was registered with European Union Drug Regulating Authorities ClinicalTrials EudraCT, number 2015-001329-17, and with ClinicalTrials.gov, number NCT02608437.

Clinical procedures

The study followed a traditional 3 + 3 design. The first cohort received guadecitabine 30 mg/m^2/day subcutaneously on days 1 to 5 every 3 weeks (q3w) starting on week 0 for a total of four cycles (weeks 0, 3, 6, and 9), and ipilimumab 3 mg/kg intravenously over 90 minutes starting on day 1 of week 1 q3w for a total of four cycles (weeks 1, 4, 7, and 10). The dose-limiting toxicity (DLT) observation period was defined as the first 3 weeks of treatment, that is, from day 1 to day 21 of cycle 1. In the absence of DLTs, the dose of guadecitabine was escalated per protocol to 45 mg/m^2/day; as no DLTs were observed at this dose level in the initial six patients enrolled, the study protocol was amended in order to allow a further escalation of guadecitabine to 60 mg/m^2/day. If one DLT occurred in the first three patients of any cohort, an additional three patients were enrolled at the same dose level. If two or more DLTs were encountered in a single cohort, the previous lower dose level was evaluated. DLT was defined as any of the following events occurring during the first treatment cycle

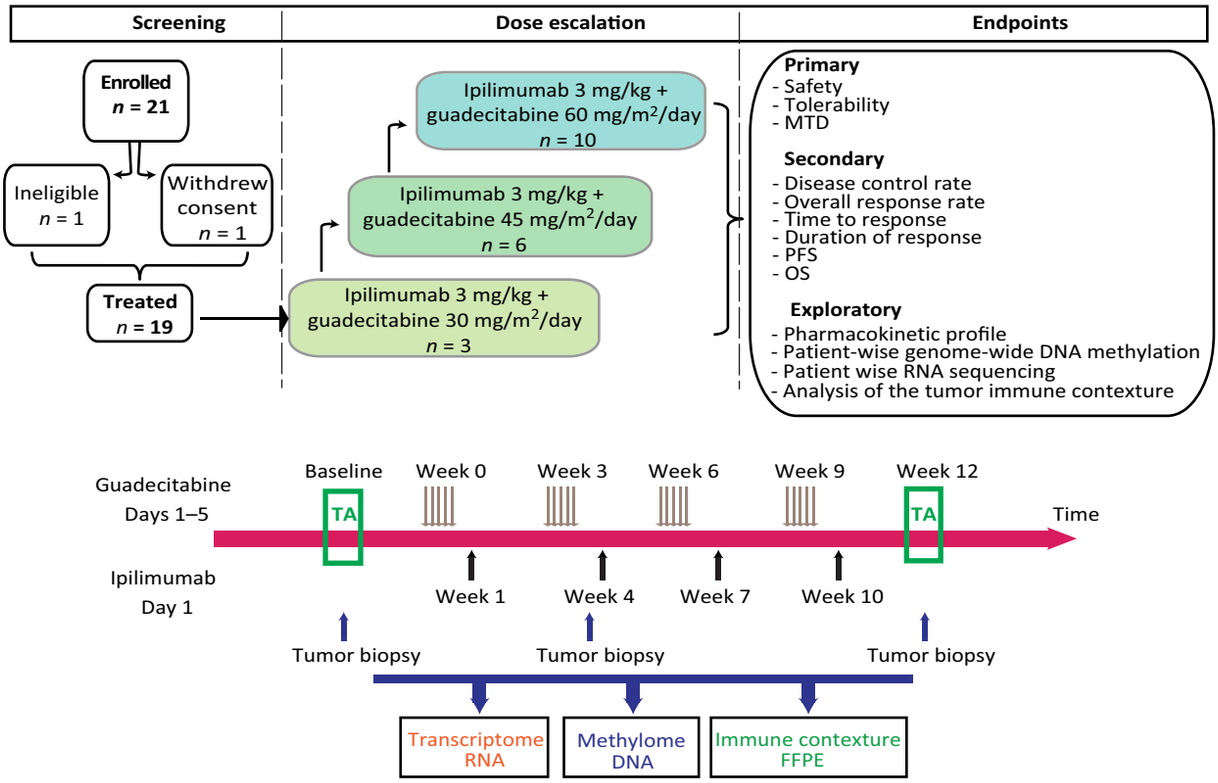

Figure 1.

NIBIT-M4 study design. Patients with unresectable stage III or IV cutaneous melanoma received four cycles of guadecitabine (days 1–5 every 21 days) and four cycles of ipilimumab (day 1 every 21 days). Tumor was assessed (TA) at baseline, at week 12, week 18, and week 24, and every 12 weeks thereafter. Tumor biopsies were taken at baseline, week 4, and week 12.

and clearly related to study treatment: grade 4 neutropenia; febrile neutropenia grade $\geq$3; platelet count <25,000/L or thrombocytopenic bleeding; alanine aminotransferase or aspartate aminotransferase grade $\geq$3 for 7 days; any grade 3 or 4 nonhematologic toxicity (excluding alopecia, nonpremedicated nausea and vomiting); grade 3 or 4 clinically significant nausea, vomiting, or diarrhea in the presence of maximal supportive care; or interruption of treatment >2 weeks due to toxicity. Patients in whom toxicity failed to resolve to grade $\leq$2 after 14 days off treatment were removed from the study. The MTD was defined as the highest guadecitabine dose level in combination with ipilimumab at which no more than one of six patients experienced a DLT. Once the MTD was established, additional patients were treated at that dose up to a total of 19 patients overall. A Safety Monitoring Committee established for the trial monitored safety and reviewed all reported adverse event (AE) and serious AEs on an ongoing basis throughout the trial. Safety was continuously evaluated according to the National Cancer Institute Common Terminology Criteria for Adverse Events, version 4.0. Safety assessments included medical review of AE reports and clinical assessment of vital signs, physical examinations, and clinical laboratory tests.

Radiological (MRI or CT scans of brain, bone, chest, abdomen, pelvis, and other soft tissue, as applicable) and photographic (skin lesion) tumor assessments were performed at baseline, at weeks 12, 18, and 24, and then every 12 weeks for all nonprogressing subjects. At each evaluation, investigators assessed the objective response rate [ORR; complete response (CR), partial response (PR), stable disease (SD), or progression disease (PD)] as categorized by immune-related (ir) response criteria (21). Unless the patient was rapidly deteriorating, PD was confirmed by two scans at least 4 weeks apart. The pharmacokinetic profiles of guadecitabine and active metabolite decitabine were characterized by analysis of K_2EDTA-treated plasma by validated (22, 23) liquid chromatography-mass spectrometry/mass spectrometry, using tetrahydrouridine for stabilization and with linear assay ranges of 1 to 200 ng/mL for guadecitabine and 0.5 to 100 ng/mL for decitabine. Plasma samples were collected on day 1 of the first guadecitabine cycle. Samples were collected before dosing and at 15, 30, 60, and 90 minutes, and 2, 4, 6, and 8 hours after the dose.

Clinical endpoints

The primary endpoint was the MTD and safety of guadecitabine combined with ipilimumab. Secondary ir endpoints included ir-disease control rate (DCR; confirmed ir-CR, -PR, or -SD), ir-ORR (ir-CR or -PR), time to response, duration of response, and progression-free survival (PFS; time between first dose and progression of existing lesions or the occurrence of new lesions); OS was also assessed. Exploratory endpoints included the pharmacokinetic profile of guadecitabine and decitabine at cycle 1 day 1, patient-wise genome-wide DNA methylation and RNA sequencing, and analysis of the tumor immune contexture using neoplastic samples obtained by surgical removal or fine-needle biopsy at baseline, week 4, and week 12.

Isolation of total DNA

A maximum amount of 25 mg of frozen tissue was placed in 1.5-mL microcentrifuge tubes containing 600 μL of Buffer RTL Plus and homogenized using the TissueLyser (Qiagen) for 1.5 minutes at 28 Hz. The position of TissueLyser set adapter was inverted to give uniform disruption and homogenization of the sample. Sample disruption was carried out at 4°C after storing the adapter set at -80°C for at least 2 hours. Genomic DNA was extracted using the QIAamp DNA Mini Kit (Qiagen) according to the manufacturer's protocol. DNA concentration and quality were determined using the NanoDrop ND-1000 UV-Vis Spectrophotometer (NanoDrop Technologies, Thermo Fisher Scientific).

Library preparation and sequencing

For reduced representation bisulfite sequencing (RRBS), 100 ng of genomic DNA were digested for 6 hours at 65°C with 20 U TaqI (New England Biolabs) and for 6 hours at 37°C with 20 U of MspI (New England Biolabs) in 30 μL of 1x NEB buffer 2. To retain even the smallest fragments and to minimize loss of material, end preparation and adaptor ligation were performed in a single-tube setup. End fill-in and A-tailing were performed by addition of Klenow Fragment 3′ & gt; 5′ exo- (New England Biolabs); and dNTP mix (10 mmol/L dATP, 1 mmol/L dCTP, 1 mmol/L dGTP). After ligation to methylated Illumina TruSeq LT v2 adaptors using T4 DNA Ligase rapid (Enzymatics), the libraries were size selected by performing a 0.75x clean-up with AMPure XP beads (Beckman Coulter). The libraries were pooled based on qPCR data and subjected to bisulfite conversion using the EZ DNA Methylation Direct Kit (Zymo Research) with changes to the manufacturer's protocol: conversion reagent was used at 0.9x concentration, incubation performed for 20 cycles of 1 minutes at 95°C and 10 minutes at 60°C, and the desulphonation time was extended to 30 minutes. These changes increase the number of CpG dinucleotides covered, by reducing double-strand break formation in larger library fragments. Bisulfite-converted libraries were enriched using APA HiFi HS Uracil+ RM (Roche). The minimum number of enrichment cycles was estimated based on a qPCR experiment. After a 1x AMPure XP clean-up, library concentrations were quantified with the Qubit Fluorometric Quantitation system (Life Technologies), and the size distribution was assessed using the Bioanalyzer High Sensitivity DNA Kit (Agilent). Reduced representation sequencing libraries were sequenced on Illumina HiSeq 3000/4000 instruments in 50-base-pair-single-end mode; base calls provided by the Illumina Real-Time Analysis software were subsequently converted into BAM format (Illumina2bam) before demultiplexing (BamIndexDecoder) into individual, sample-specific BAM files via Illumina2bam tools (1.17.3 https://github.com/wtsi-npg/illumina2bam), as previously described (24).

RRBS data processing

Read sequences were trimmed using Trimmomatic (https://github.com/timflutre/trimmomatic) with the following settings: ILLUMINACLIP:RRBS_adapters.fa:2:40:7 SLIDINGWINDOW:4:15 MAXINFO:20:0.50 MINLEN:18. Reads were aligned to the GRCh38 assembly of the human genome, using BSMAP (https://www.ncbi.nlm.nih.gov/pubmed/19635165) in its RRBS mapping mode. To avoid bias in the global methylation rates arising from differences in the sequencing depth, RRBS data were downsampled to 10 million reads in each sample. DNA methylation levels for individual CpGs were calculated using custom Python scripts. Bisulfite conversion efficiency was estimated by aligning unmapped reads to the spike-in genome for methylated or unmethylated control sequences. CpGs located in repetitive regions according to the UCSC RepeatMasker track were excluded from further analysis.

DNA methylation analyses

To analyze the global methylation states, methylKit (25) and custom R scripts were used. Raw methylation level data on CpG sites were filtered such that only sites with a read coverage >10 and having a coverage not higher than the 99.9 percentile of all sites were retained. Furthermore, only CpG sites that were present in all samples (baseline, week 4, week 12) of an individual patient and had a reliable measurement methylation level were used for further analyses. To statistically test the methylation levels at each CpG site, we calculated *P* values as previously described (26). Sites with a probability of $P < 0.05$ that their real methylation level lies outside a 0.1 error interval were considered reliable. Global methylation levels were calculated as mean and median methylation level of all retained CpG sites and plotted as density (beta-binomial distribution) and box plots using ggplot2 (27). A Wilcoxon signed-rank test with continuity correction was used to calculate *P* values for comparing methylation level distribution at different time points.

Isolation of total RNA and sequencing

Total RNA was extracted by TRIzol Reagent (Thermo Fisher Scientific). Frozen tissue was placed in 2-mL microcentrifuge tubes containing 1-mL TRIzol reagent and homogenized using the TissueLyser (Qiagen) for 1.5 minutes at 28 Hz, as for DNA isolation. Total RNA extraction was done as previously described (28). Quantity and quality of RNA extracted were assessed by NanoDrop ND-1000 UV-Vis Spectrophotometer (NanoDrop Technologies, Thermo Fisher Scientific) and by Agilent 2100 Bioanalyzer (Agilent Technologies) using the expert eukaryote Total RNA kit (Agilent).

Library preparation and sequencing

The amount of total RNA was quantified using the Qubit Fluorometric Quantitation system (Life Technologies), and the RNA integrity number was determined using the Experion Automated Electrophoresis System (Bio-Rad). RNA sequencing libraries were prepared with the TruSeq Stranded mRNA LT sample preparation Kit (Illumina) using both Sciclone and Zephyr liquid handling robotics (PerkinElmer). Library concentrations were quantified with the Qubit Fluorometric Quantitation system (Life Technologies), and the size distribution was assessed using the Experion Automated Electrophoresis System (Bio-Rad). For sequencing, samples were diluted and pooled into NGS libraries in equimolar amounts, as previously described (29).

Sequencing and raw data processing

Expression profiling libraries were sequenced on Illumina HiSeq 3000/4000 instruments in 75-base-pair-paired-end mode, and base calls provided by the Illumina Real-Time Analysis software were subsequently converted into BAM format (Illumina2bam) before demultiplexing (BamIndexDecoder) into individual, sample-specific BAM files via Illumina2bam tools (1.17.3 https://github.com/wtsi-npg/illumina2bam), as previously described (29).

RNA-seq data analysis

BAM files were converted to FASTQ files with "bam2fastx." FASTQ files were preprocessed with Trimmomatic (30) to remove adapter sequences, trim read ends with a Phred quality lower than 20, and discard reads shorter than 36 bp. The preprocessed reads were mapped to the GRCh38 human genome with the STAR aligner (31) using the default parameter settings. Gene counts were computed with htseq-count (32) considering reads mapping to all exons of a gene ("-t exon" and "-i gene_name" options) on the correct strand ("-s reverse" option). EdgeR (33) was used to identify differentially expressed genes (DEG) at week 4 and week 12 compared with baseline for each single patient, after removal of genes with less than five counts across all libraries and normalization with the trimmed-mean of M-values approach (34). Genes with an FDR-corrected P value <0.05 and an absolute $\log_2$ fold change greater than 1 were selected as differentially expressed. EdgeR was also used to test DEG in responding versus nonresponding patients at baseline, week 4, and week 12. For this analysis, count data from technical replicates (i.e., different sequencing runs of the same sample) were summed, filtered for genes with less than five counts across all samples, subjected to trimmed-mean of M-values normalization, and tested for differential gene expression with EdgeR. For each time point, all genes with uncorrected P values < 0.05 were selected for ingenuity pathway analysis (IPA) Knowledge Base analysis, performed considering the uncorrected P values and $\log_2$ fold change computed with EdgeR. Log_2 fold changes were used to assess significant activation or inhibition Z-scores for each process. A negative log P value was also assigned to the pathways based on a Fisher exact test of the probability of the number of genes included in the given pathways, and by the probability that the association between the query genes and the canonical pathway was due to chance alone. Modulation, activation, and inhibition scores of canonical pathways were calculated counting the number of tumor samples for which a specific pathway was modulated (P value < 0.05 and Z-score $\geq$ 2 or Z-score ≤ -2), activated (P value < 0.05 and Z-score $\geq$ 2), or inhibited (P value < 0.05 and Z-score ≤ -2), at week 4 or week 12 compared with baseline. The percentages of activation or inhibition were calculated as the ratio between the activation or inhibition, respectively, and the modulation score.

IHC analysis

Serial 3-μm formalin-fixed paraffin-embedded tissue sections were stained using an AutostainerPlus (Dako). Antigen retrieval and deparaffinization were carried out on a PT-Link (Dako) using the EnVision FLEX Target Retrieval Solutions (Dako). Endogenous peroxidase and nonspecific staining were blocked with H_20_2 3% (Gifrer, 10603051) and Protein Block (Dako, X0909), respectively. The primary antibodies used were: anti-CD8 clone C8/144B and anti-CD20 clone L26 (Dako), anti–PD-1 clone EH33 (CoStim), and anti-HLA class I clone EMR8-5 (Abcam); the secondary antibody was an horseradish peroxidase–labeled anti-mouse Ig (Dako). Peroxidase activity was detected using 3-amino-9-ethylcarbazole substrate (Vector Laboratories, SK-4200). All stained slides were digitalized with a NanoZoomer scanner (Hamamatsu). The density (cells/mm^2) of CD8$^+$ and PD-1$^+$ T cells, and of CD20$^+$ B cells, in the tumor core was digitally quantified with Calopix software (Tribvn), and the percentage of tumor cells expressing HLA class I was quantified with Halo software (Indica Labs).

Statistical analysis

The safety analysis population included all patients who received at least one dose of drug. All safety parameters were summarized and presented in tables based on this population. With the aim of excluding a combination with an activity in terms of ir-DCR lower than 15%, a total of 19 patients will be considered; if no ir-DCR are observed, the study will be terminated as negative because there is a probability lower than 5% ($P = 0.046$) of observing no ir-DCR in 19 patients if the true ir-DCR is 15% or higher. For ir-DCR and ir-ORR, two-sided 95% confidence intervals (CIs) were calculated using the exact method based on binomial distribution. Descriptive statistics were used for ir time to response and patient demographics and characteristics. Statistical analyses were performed using Statistical Package for the Social Sciences software, version 21.0.

To select and compare methylated CpG sites, several filters were imposed on the raw methylation data. First, sites were required to have a minimum coverage of over 10 reads and a coverage not higher than the 99.9 percentile of all sites. Secondly, CpG were required to be present in all samples (baseline, week 4, week 12) from an individual patient. Last, the CpG sites were required to have a probability of $P < 0.05$ that their real methylation level lay outside an error interval of 0.1. Each patient was analyzed separately, and the significant difference between global methylation level distributions was assessed by a Wilcoxon signed-rank test with continuity correction. Significance in median methylation level (all matching significant sites in an individual patient) between different time points was also assessed by Wilcoxon signed-rank test. Differential gene expression at week 4 and week 12 with respect to the baseline in individual patients was tested on RNA sequencing data with EdgeR (33), using a cutoff of 0.05 on FDR-corrected P values and 1 on absolute $\log_2$ fold changes. EdgeR was also used to identify DEG between responder and nonresponder patients selected imposing a significance threshold of 0.05 on FDR-corrected P values. Significant differences between IHC data across related samples were obtained by Friedman test or by Mann–Whitney test when IHC data were integrated with patient's response.

Results

Patient characteristics and treatment exposure

Twenty-one patients with metastatic melanoma were enrolled, one patient was ineligible, and another withdrew the consent to the study (Fig. 1). Nineteen patients were treated with different dose levels of guadecitabine combined with ipilimumab and were evaluable for safety and efficacy (data cutoff January 30, 2019). In detail, guadecitabine was administered at 30 mg/m^2/day in the first three patients (cohort 1), at 45 mg/m^2/day in the following six patients (cohort 2), and, following a protocol amendment (see Clinical Procedures), at 60 mg/m^2/day in the last 10 patients (cohort 3). Baseline characteristics are shown in Table 1. Eighteen patients (95%) were treatment-naïve at study entry, and one (5%) had received one line of therapy for locally advanced disease. Two patients (13%) had unresectable stage III, 11 (58%) had stage M1a, one (5%) had stage M1b, and five (26%) had stage M1c metastatic melanoma. Seventeen (89%) patients completed all four cycles of guadecitabine followed by ipilimumab, one died during treatment due to disease progression, and one discontinued after two cycles of therapy due to the development of symptomatic brain metastases requiring steroids and radiotherapy.

Table 1. Patient cohorts, demographics, and baseline characteristics

	Cohort 1 Guadecitabine 30 mg ($n = 3$)[a]	Cohort 2 Guadecitabine 45 mg ($n = 6$)	Cohort 3 Guadecitabine 60 mg ($n = 10$)	All patients ($n = 19$)
Age (y)	59 (27–82)[b]	59 (43–86)	56 (49–78)	58 (27–86)
Gender				
Male	2 (67%)[c]	6 (100%)	9 (90%)	16 (84%)
Female	1 (33%)	0	1 (10%)	3 (16%)
ECOG performance status				
0	2 (67%)	5 (83%)	9 (90%)	16 (84%)
1	1 (33%)	1 (17%)	1 (10%)	3 (16%)
M Stage at study entry				
M0 (unresectable stage III)	0	2 (33%)	0	2 (11%)
M1a	2 (67%)	3 (50%)	6 (60%)	11 (58%)
M1b	0	0	1 (10%)	1 (5%)
M1c	1 (33%)	1 (17%)	3 (30%)	5 (26%)
LDH				
≤ULN	3 (100%)	5 (83%)	8 (80%)	16 (84%)
≥ULN	0	1 (17%)	2 (20%)	3 (16%)
BRAF status				
Mutant	2 (67%)	2 (33%)	1 (10%)	5 (26%)
WT	0	4 (67%)	9 (90%)	13 (69%)
Unknown	1 (33%)	0	0	1 (5%)
Prior lines of metastatic therapy				
0	3 (100%)	5 (83%)	10 (100%)	18 (95%)
1	0	1 (17%)	0	1 (5%)

Abbreviations: ECOG, Eastern Cooperative Oncology Group; LDH, lactate dehydrogenase; ULN, upper limit of normal.
[a]Number of treated patients per cohort.
[b]Median (range).
[c]*n* (%).

Safety

All 19 (100%) patients had AEs of any grade, which were grade 3 or 4 in 16 (84%) patients (Table 2). Treatment-related AEs of any grade were observed in 18 (95%) patients, and grade 3 or 4 events in 15 (79%) patients (Table 2). The most common treatment-related AEs of any grade were myelotoxicity in 17 (89%) patients, and ir-AEs in 12 (63%) patients. Myelotoxicity events were grade 3 or 4 in 79% of cases (Table 2) and were more frequent in patients treated with guadecitabine 60 mg/m^2/day (Table 3); no febrile neutropenia was observed. All ir-AEs were grade 1 or 2 and were most commonly skin or gastrointestinal toxicities (Table 2). No DLTs were observed at any investigated dose of guadecitabine. Treatment-related AEs and ir-AEs were generally manageable and reversible as per protocol management guidelines. One (14%) patient with grade 2 ir-colitis required steroid treatment; grade 3 or 4 myelotoxicity was treated with growth factors and prophylactic antibiotics. Median time to resolution of treatment-related grade 2–4 AEs and of ir grade 1–2 AEs was 7 days (range, 1–45 days) and 7 days (range, 4–9 days), respectively.

Table 2. Summary of AEs

	Cohort 1 Guadecitabine 30 mg ($n = 3$)[a]		Cohort 2 Guadecitabine 45 mg ($n = 6$)		Cohort 3 Guadecitabine 60 mg ($n = 10$)		All patients ($n = 19$)	
Event	**Any grade**	**Grade 3–4**	**Any Grade**	**Grade 3–4**	**Any Grade**	**Grade 3–4**	**Any Grade**	**Grade 3–4**
Any AE[b]	3 (100%)[c]	1 (33%)	6 (100%)	6 (100%)	10 (100%)	9 (90%)	19 (100%)	16 (84%)
Any treatment-related AE	2 (67%)	1 (33%)	6 (100%)	6 (100%)	10 (100%)	8 (80%)	18 (95%)	15 (79%)
Fatigue/asthenia	0	0	1 (17%)	0	3 (30%)	0	4 (21%)	0
Nausea/vomiting	2 (67%)	0	1 (17%)	0	1 (10%)	0	4 (21%)	0
Pain	0	0	3 (50%)	0	4 (40%)	0	7 (37%)	0
Myelotoxicity	1 (33%)	1 (33%)	6 (100%)	6 (100%)	10 (100%)	8 (80%)	17 (89%)	15 (79%)
Neutropenia	1 (33%)	1 (33%)	6 (100%)	6 (100%)	10 (100%)	8 (80%)	17 (89%)	15 (79%)
Leukopenia	1 (33%)	0	2 (33%)	1 (17%)	9 (90%)	3 (30%)	12 (63%)	4 (21%)
Thrombocytopenia	0	0	1 (17%)	0	2 (20%)	0	3 (16%)	0
Lymphocytopenia	1 (33%)	0	1 (17%)	1 (17%)	4 (40%)	0	6 (32%)	1 (5%)
Any immune-related AE	1 (33%)	0	5 (83%)	0	6 (60%)	0	12 (63%)	0
Skin and mucosal	1 (33%)	0	5 (83%)	0	6 (60%)	0	12 (63%)	0
Rash	0	0	4 (67%)	0	4 (40%)	0	8 (42%)	0
Pruritus	0	0	4 (67%)	0	4 (40%)	0	8 (42%)	0
Erythema	1 (33%)	0	2 (33%)	0	2 (20%)	0	5 (26%)	0
Injection site reaction	1 (33%)	0	0	0	0	0	1 (5%)	0
Gastrointestinal (diarrhea or colitis)	0	0	2 (33%)	0	2 (20%)	0	4 (21%)	0
Serum amylase increase	0	0	0	0	1 (10%)	0	1 (5%)	0

[a]Number of treated patients per cohort.
[b]AEs were graded using the NCI Common Terminology Criteria for Adverse Events (version 4.0).
[c]*n* (%).

Table 3. Frequency of myelotoxicity

	Cohort 1 Guadecitabine 30 mg ($n = 3$)[a]		Cohort 2 Guadecitabine 45 mg ($n = 6$)		Cohort 3 Guadecitabine 60 mg ($n = 10$)	
Event	**Any grade**	**Grade 3–4**	**Any grade**	**Grade 3–4**	**Any grade**	**Grade 3–4**
Myelotoxicity	2[b]	1	21	9	92	33
Neutropenia	1	1	18	8	58	24
Leukopenia	1	0	2	1	32	9
Thrombocytopenia	0	0	1	0	2	0
Lymphocytopenia	6	0	4	2	12	0

[a]Number of treated patients per cohort.
[b]Number of times that AEs were observed.

Clinical activity and pharmacokinetics

The ir-ORR was 5/19 (26%; 95% CI, 10.1–51.4) among them two confirmed CR and three confirmed PR, and ir-DCR was 8/19 (42%; 95% CI, 21.1–66.0); median time to response was 12 weeks and median duration of response was 25.4 months (95% CI, 10.4–40.4). At a median follow-up of 26.3 months, median PFS was 5.6 months (95% CI, 4.5–6.6) and median OS was 26.2 months (95% CI, 3.5–48.9); 1- and 2-year OS rates were 80% (95% CI, 59.2–100.0) and 56% (95% CI, 29.0–83.0), respectively.

Guadecitabine underwent efficient conversion to its active metabolite decitabine as seen by analysis of plasma exposure (data not shown); decitabine exposure as measured by AUC increased in a dose-dependent manner (Supplementary Table S1).

Immunobiological activity

To explore the immunobiological activity of guadecitabine combined with ipilimumab, serial tumor biopsies from the initial eight and 11 patients treated were analyzed for methylation and gene expression profiles, and for tumor immune contexture, respectively. The investigated tumor biopsies were derived from skin lesions, and from metastatic lymph nodes for patient 7 at week 4 and week 12. RRBS of CpG sites demonstrated a significant reduction in global methylation in investigated tumor samples at week 4 (median, 74.5%; range, 68.4–88.2; $P = 0.03$) and week 12 (median, 75.0%; range, 69.2–84.2; $P = 0.01$), compared with baseline (median, 80.3%; range, 72.7–87.8; Fig. 2; Supplementary Table S2). Patient-wise differential expression analysis of RNA sequencing data resulted in a median of 2,454 (range, 1,179–12,250) and of 4,131 (range, 2,083–12,016) DEGs at week 4 and week 12, respectively, compared with baseline (Supplementary Table S3). Medians of 49.4% (range, 17.4%–58.7%) and 53.9% (range, 41.3%–62.7%) of DEG were upregulated at week 4 and week 12, respectively (Supplementary Table S3). Of the 136 canonical pathways that were significantly modulated according to IPA ($P < 0.05$ and Z-score ≥ 2 or Z-score ≤ -2) at week 4 or week 12 compared with baseline in at least 1 patient, the most frequently activated (Z-score ≥ 2) were ir pathways (Supplementary Table S4). Specifically, iCOS-iCOSL signaling in T-helper cells, PKCθ signaling in T lymphocytes, role of NFAT in regulation of the immune response, Th1, calcium-induced T-lymphocyte apoptosis, and IFN signaling pathways were activated in at least five investigated tumor samples, with frequency of activation ranging from 56% to 71% (Supplementary Table S4).

Supervised differential expression analysis between responding and nonresponding patients identified 3,104, 3,920, and 3,796 DEG at baseline, week 4, and week 12, respectively, the majority of which were upregulated in responders (data not shown). Th1 and Th2, dendritic cell maturation, calcium-induced T-lymphocyte apoptosis, iCOS-iCOSL signaling in T-helper cell, neuroinflammation signaling, cAMP-mediated signaling, and role of NFAT in regulation of the immune response pathways were significantly ($P < 0.05$) activated (Z-score≥ 2) at baseline in responders versus nonresponders (Supplementary Fig. S1; Supplementary Table S5). The absolute number of DEG belonging to these pathways increased with treatment and peaked at week 12 (Supplementary Fig. S1); furthermore, additional ir pathways (e.g., acute phase response, B-cell receptor, NF-κB, and IL2 signaling) were activated in responders versus nonresponders at week 4 and/or week 12 (Supplementary Fig. S1; Supplementary Table S5).

IHC analysis of tumors from the first 11 patients treated demonstrated upregulated expression of HLA class I–positive melanoma cells in nine of 11 (81.8%) patients at week 4 and/or week 12 (Supplementary Table S6). In eight evaluable patients, significant correlations (Fig. 3A and B) were found between the expression of HLA class I molecules by IHC (Fig. 3A) and RNA sequencing expression of *HLA-A*, *-B*, and *-C* (Friedman test $P < 1e\text{-}05$) and *B2M* (Friedman test $P < 1e\text{-}05$) genes (Fig. 3B). Representative results of IHC staining for HLA class I in tumor samples from patients 2 and 3 (Supplementary Table S6) are shown in Fig. 3C. An upregulated expression of HLA class II loci (i.e., DPA1, DPB1, DQA1, DQA2, DQB1, DRA, DRB1) was identified by RNA-seq in tumor biopsies from seven of eight (87.5%) patients at week 4 and/or week 12 (data not shown). $CD8^+$ T-cell density in the tumor core was higher at week 12 (median, 586.9/mm^2; range, 107.5–1257.3) than at baseline (median, 262.7/mm^2; range, 9.1–1460.0; Fig. 4A; Supplementary Table S7), and was also higher in responding compared with nonresponding patients at all time points investigated (Fig. 4C). Similar results were observed for PD-1^+ T cells (Fig. 4B and D; Supplementary Table S7) and for $CD20^+$ B cells (Supplementary Fig. S2; Supplementary Table S7). Figure 4E and F shows representative results of the IHC staining for $CD8^+$ and PD-1^+, respectively, in tumor samples from patients 2 and 11.

Discussion

In this phase Ib study, treatment of patients with metastatic melanoma with guadecitabine combined to the standard ipilimumab regimen was safe and tolerable, and had promising tumor immunomodulatory and clinical activities, worth to be explored further. The starting dose of 30 mg/m^2/day of guadecitabine, though being only the 33% of the MTD for single-agent treatment in patients with myeloid malignancies (35), was selected because it was planned to be administered for the first time on a 21-day/cycle compared with its conventional administration on a 28-day/cycle (35), and we wanted to be cautious about potential side effects with this new schedule of administration and its association with ipilimumab. In

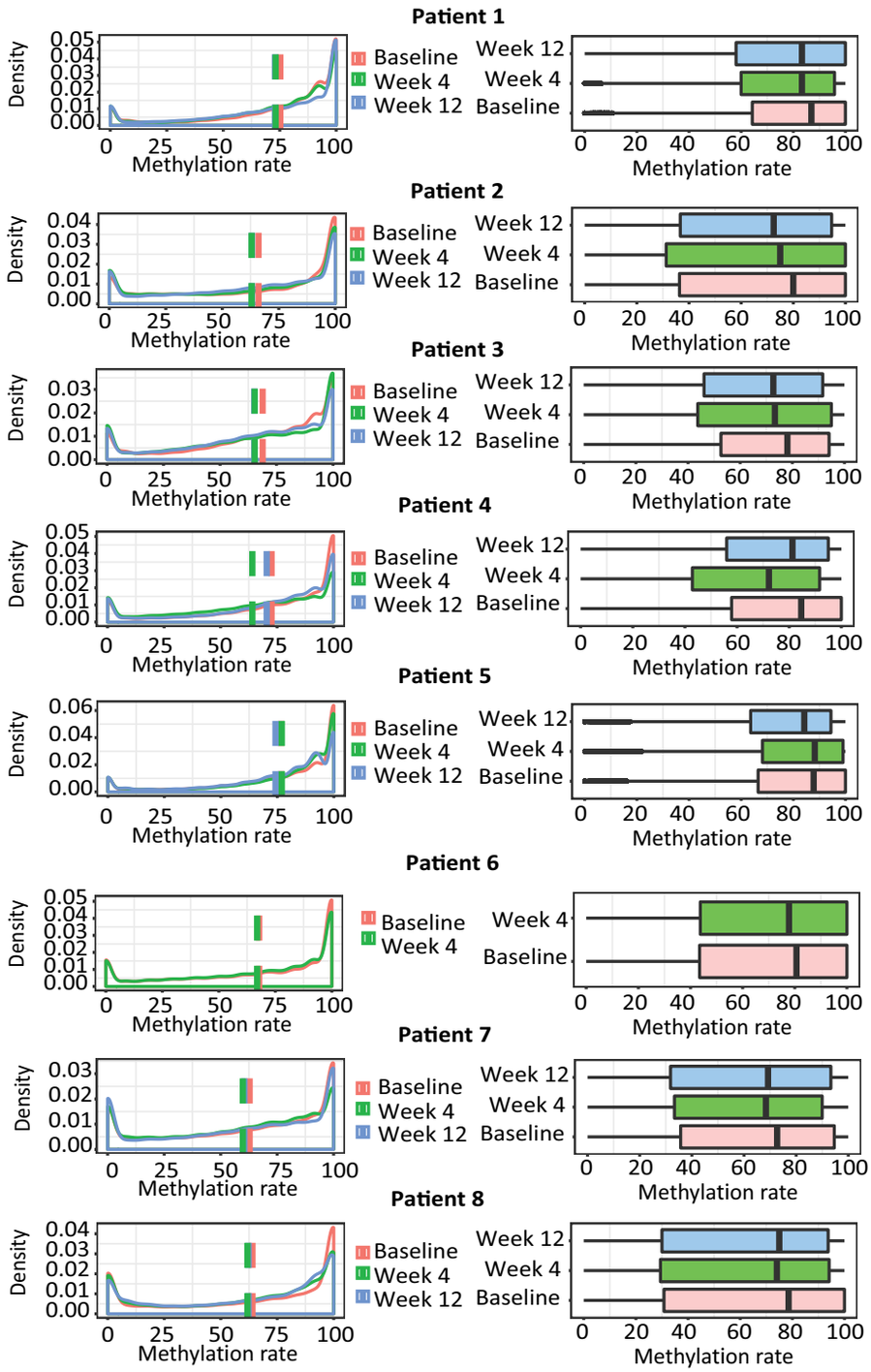

Figure 2.
Global DNA methylation analysis of tumor samples. DNA extracted from tumors of the first eight patients was used to measure global methylation by RRBS. Analyses were done in baseline (pink), week 4 (green), and week 12 (blue) lesions of a patient, and only CpG sites with a minimum coverage of single site >10 and *P* value of the methylation level <0.05 were considered. Data are represented as patient-wise density plots (with corresponding mean values, dotted colored lines) and boxplot (with corresponding median values, solid black lines).

addition, preliminary information we had available at the study protocol was drafted, suggested for a lower MTD of guadecitabine in solid tumors as compared with myeloid malignancies. For these reasons, the initial study protocol foresaw a single escalation to 45 mg/m^2/day in case no DLTs were observed at 30 mg/m^2/day. As we did not observe DLTs also in the initial six patients treated at 45 mg/m^2/day, the study was formally amended allowing a further escalation at 60 mg/m^2/day of guadecitabine, in which all the remaining patients were enrolled. No maintenance therapy with guadecitabine and/or ipilimumab was planned in the NIBIT-M4 study. The decision not to have maintenance with ipilimumab was due to the willingness to use it according to its standard-of-care administration in patients with melanoma. On the other hand, maintenance with guadecitabine was excluded because no information was available on its potential long-term toxicity

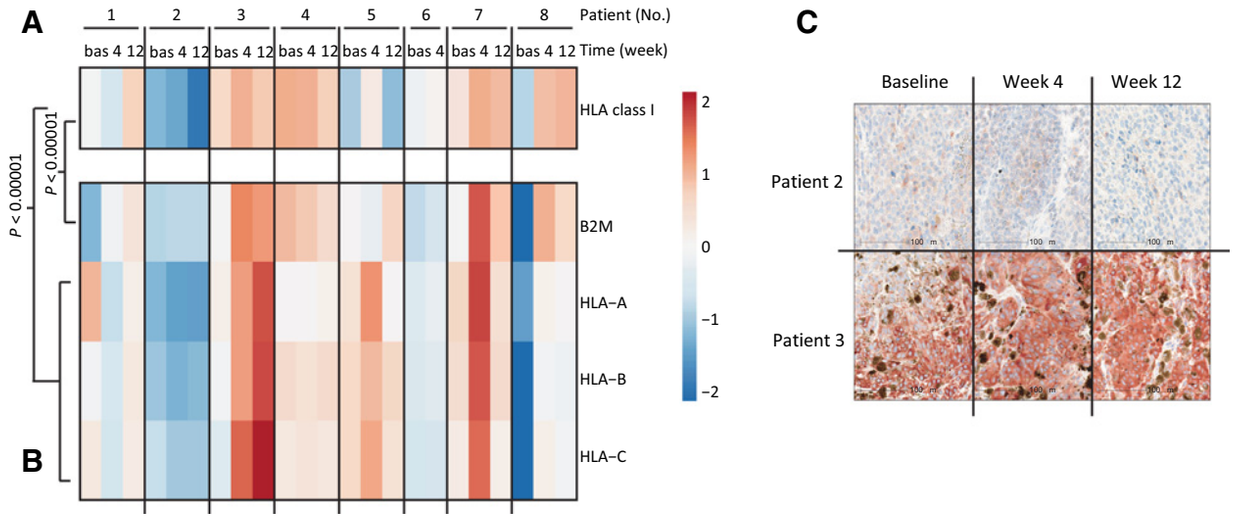

Figure 3.

HLA class I expression in tumor samples. Heat-map representing HLA class I proteins (**A**) and the relative expression of *HLA-A*, *HLA-B*, and *HLA-C*, and of *B2M* genes (**B**) at baseline (bas), week 4 (4), and week 12 (12). Correlation between IHC (**A**) and RNA sequencing gene expression levels (log-scale, **B**) were assessed by Friedman test. The heat-map was computed from Z-scores of gene expression and IHC values. Chromogenic IHC with antibody targeting HLA class I in tumors from representative patients at different time points (skin metastases) during treatment (**C**).

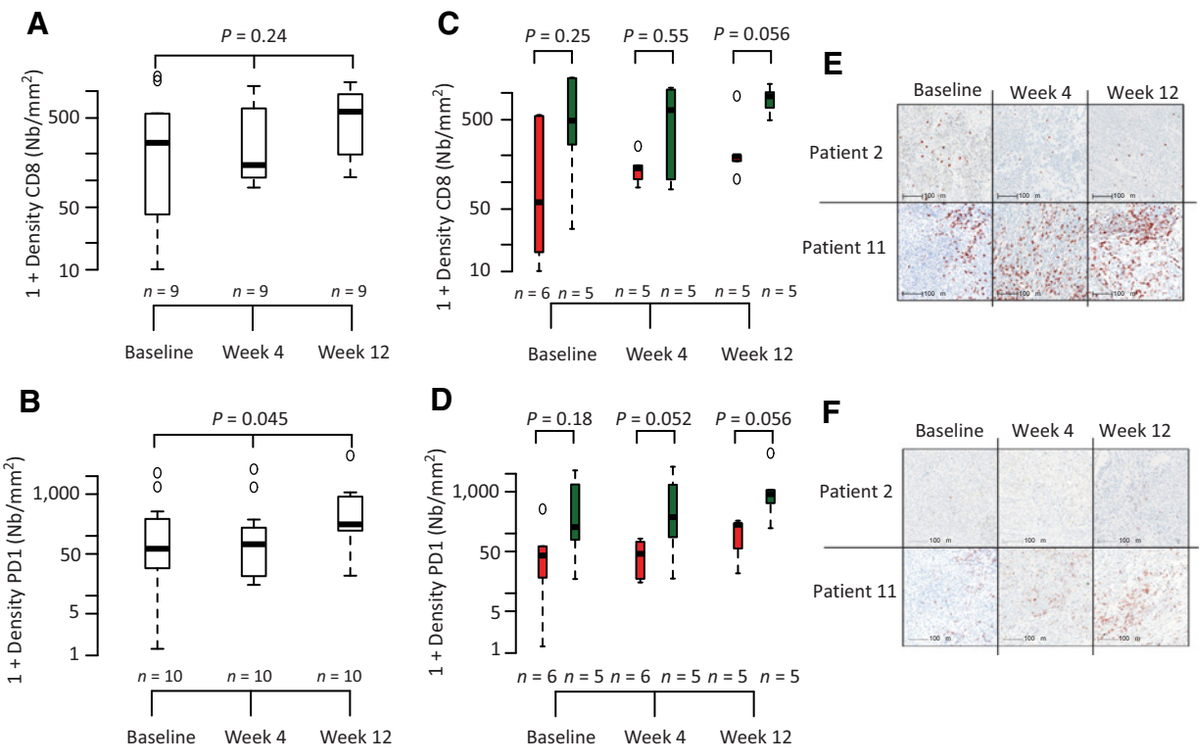

Figure 4.

Modulation of tumor immune contexture. The density of $CD8^+$ (**A**) and of PD-1^+ (**B**) T cells was investigated by IHC in tumor cores of melanoma sections at baseline, week 4, and week 12 and analyzed by Friedman test. $CD8^+$ (**C**) and PD-1^+ (**D**) T-cell densities were correlated with clinical outcome (red boxplot = patients with progressive disease; green boxplot = patients with disease control) by Mann–Whitney test. Quantification of scanned slides was performed using Calopix software (Tribvn). Chromogenic IHC with antibody targeting $CD8^+$ (**E**) and PD-1^+ (**F**) cells in tumor cores from representative patients at different time points (skin metastases) during treatment.

in patients with solid tumors at the time the study was activated. Nevertheless, based on the comprehensive results of the NIBIT-M4 study, it cannot be excluded that maintenance with guadecitabine and/or ipilimumab is worth to be explored in further studies.

Treatment was safely administered to patients at all doses of guadecitabine investigated, without DLT. Grade 3 or 4 myelotoxicity, the most commonly observed AE, was more frequent at the highest dose level of guadecitabine (60 mg/m^2/day). Although this dose was less well tolerated, its toxicity was manageable and reversible, and all patients received the full course of treatment. Guadecitabine 60 mg/m^2/day for 5 days in a 28-day cycle is the established dosing regimen in myeloid malignancies, and it is interesting that the same dose/day was tolerated in this previously unexplored 21-day cycle, which was chosen to enable treatment of guadecitabine combined with the approved 3-weekly schedule of ipilimumab. A lower rate of known irAEs was observed in treated patients; whether guadecitabine may account for such observation and its potential mechanism(s) of action remain to be investigated. No AEs other than those typically reported with guadecitabine (35) or ipilimumab (11) monotherapy were observed, including no unexpected or potentially additive toxicities, thus supporting the feasibility of the explored therapeutic sequence at all doses of guadecitabine investigated. In contrast, severe myelosuppression was reported in several other studies of guadecitabine in solid tumors (36–38), leading to lower MTDs of 30–45 mg/m^2/day. In the ovary and colorectal studies (37, 38), coadministration of guadecitabine with myelosuppressive chemotherapy undoubtedly affected overall tolerability, suggesting additive toxicity, unlike our results using the combination of guadecitabine and checkpoint blockade.

Of note, exposure to decitabine generated from guadecitabine, as assessed by AUC_{inf}, was lower in our study than that observed in ovarian cancer (38) and hepatocellular carcinoma (36), but was comparable with exposure previously reported for myeloid malignancies (35) and colorectal cancer (37).

The clinical efficacy of treatment is clearly beyond the scope of this phase Ib trial; the observed ir-ORR (26%) and the ir-DCR (42%) may be influenced by the high number of stage III or stage M1a subjects enrolled, due to the necessity to grant serial tumor biopsies to be available and in sufficient amount, to perform the translational studies required to understand the modifications at tumor level induced by therapy at different time points. Further studies are thus required to explore the clinical activity of the therapeutic combination investigated in this study.

Genome-scale analysis of DNA methylation of tumor samples demonstrated a broad demethylating effect of guadecitabine at both week 4 and week 12 compared with pretreatment levels. Consistent with results previously reported in hematologic malignancies (35), the demethylating activity was somewhat heterogeneous between investigated samples. RNA sequencing data analysis revealed that ir pathways were preferentially activated by treatment; frequent activation of pathways linked to T-cell function/activation suggested intratumoral enhancement of the T-cell compartment. Although the relative contributions of guadecitabine and ipilimumab to this finding cannot be unequivocally dissected, CTLA-4 blockade probably plays an active role due to its effect on T-cell function. On the other hand, upregulation of HLA class I molecules observed on melanoma cells in the majority of investigated tumor samples corroborates their established upregulation previously reported *in vitro* (28) and in syngeneic mouse models (18) with various DHAs, including guadecitabine (8, 19).

Controversial results have been recently reported on the functional role of HLA class I molecules expressed by tumor cells in the course of immune checkpoints blockade in melanoma. In one study, cell surface loss of HLA class I due to a *B2M* gene mutation was suggested to generate resistance to treatment with the anti–PD-1 pembrolizumab (39), whereas in another study, partial or complete loss of HLA class I molecules expression by neoplastic cells was not predictive of resistance to the anti–PD-1 nivolumab (17). These findings demonstrate that additional studies are required to fully understand the functional role of HLA class I molecules expression on neoplastic cells in the course of PD-1 blockade. Opposite to their debated role in the course of PD-1 therapy, more univocal evidence seems to be available concerning the functional relevance of HLA class I molecules in the course of CTLA-4 blockade therapy. Indeed, multiple molecular mechanisms, which can be also independent from *B2M* gene alterations, have been reported to drive loss or downregulation of HLA class I molecules expression on melanoma cells (40), generating a reduced effectiveness of therapy with ipilimumab (40, 41). In this scenario, the upregulation of HLA class I molecules expression on melanoma cells induced by treatment in our NIBIT-M4 study seems to suggest that combined treatment with guadecitabine and ipilimumab may contribute to improve the clinical efficacy of CTLA-4 blockade.

We also found that the IFN gamma signaling pathway was among those most frequently activated by treatment. This is of interest given the involvement of IFN gamma in host–tumor interactions (42) and also because loss of IFN gamma signaling in tumor cells may be a mechanism of tumor resistance to therapeutic CTLA-4 blockade (43).

An increase in CD8$^+$ T-cell infiltration in tumor samples has been reported in patients treated with anti–CTLA-4, though no correlation with the clinical outcome was found (44, 45). In our study, the analysis of tumor contextures showed an increase in median values of CD8$^+$, PD-1$^+$ T-cell densities at week 12, but not at week 4, compared with baseline specimens, suggesting that longer exposure to guadecitabine and ipilimumab may be required to generate high levels of tumor-infiltrating CD8$^+$ T cells. Of note, median values of CD8$^+$ and PD-1$^+$ T-cell densities were higher in responding compared with nonresponding patients at both week 4 and week 12, as well as in baseline tumor specimens. Taken together, these findings suggest that treatment with guadecitabine and ipilimumab can shift tumor T-cell distribution in the majority of patients, although a higher initial level of tumor T-cell infiltration may help therapy to achieve more rapidly an effective antitumor activity. Further supporting differential modulation of the tumor environment by treatment, supervised analysis demonstrated higher B-cell densities and activation of canonical pathways in responding compared with nonresponding patients.

To the best of our knowledge, this study provides the first evidence in patients with cancer of the immunologic activity of guadecitabine followed by ipilimumab, which seems more pronounced in patients achieving disease control. Although the limited number of patients precludes any conclusive statement on the potential of the combination, results of the NIBIT-M4 trial support the working hypothesis of this study, suggesting that a DHA-based immunocombination strategy is worth pursuing in

further clinical studies aimed at improving the efficacy of immune checkpoint inhibitors.

Disclosure of Potential Conflicts of Interest

A.M. Di Giacomo is an advisory board member/unpaid consultant for Bristol-Myers Squibb, Pierre Fabre, MSD, and Incyte. A. Covre and S. Coral are listed as co-inventors on a provisional patent application 2014/128245 on a method of treating cancer comprising administering a combination of a DNA hypomethylating agent and at least one immunomodulatory agent and/or one targeted therapy agent, that is owned by M. Maio, A. Covre, and S. Coral. A. Anichini reports receiving speakers bureau honoraria from Bristol-Myers Squibb. C. Bock reports receiving other remuneration from Diagenode s.a. M. Azab is an employee/paid consultant for Astex Pharmaceuticals. W.H. Fridman is an employee/paid consultant for Astra Zeneca, Adaptimmune, Catalym, OOSE Immunotherapeutics, and Novartis, and reports receiving speakers bureau honoraria from Bristol-Myers Squibb. Z. Trajanoski reports receiving speakers bureau honoraria from Roche, Merck, and Boehringer Ingelheim. M. Maio is listed as a co-inventor on a provisional patent application 2014/128245 on a method of treating cancer comprising administering a combination of a DNA hypomethylating agent and at least one immunomodulatory agent and/or one targeted therapy agent, that is owned by M. Maio, A. Covre, and S. Coral, and is an advisory board member/unpaid consultant for Bristol-Myers Squibb, Merck Sharp Dohme, Incyte, Astra Zeneca, GlaxoSmithKline, Merck Serono, and Roche. No potential conflicts of interest were disclosed by the other authors.

Authors' Contributions

Conception and design: A.M. Di Giacomo, A. Covre, M. Maio
Development of methodology: A.M. Di Giacomo, A. Covre, F. Finotello, D. Rieder, C. Bock, W.H. Fridman, C. Sautes-Fridman, Z. Trajanosky, M. Maio
Acquisition of data (provided animals, acquired and managed patients, provided facilities, etc.): A.M. Di Giacomo, A. Covre, R. Danielli, M. Valente, O. Cutaia, C. Fazio, G. Amato, A. Lazzeri, S. Monterisi
Analysis and interpretation of data (e.g., statistical analysis, biostatistics, computational analysis): A.M. Di Giacomo, A. Covre, F. Finotello, D. Rieder, L. Sigalotti, D. Giannarelli, F. Petitprez, L. Lacroix, C. Miracco, S. Coral, A. Anichini, C. Bock, A. Oganesian, M. Azab, J. Lowder, W.H. Fridman, C. Sautes-Fridman, Z. Trajanoski, M. Maio
Writing, review, and/or revision of the manuscript: A.M. Di Giacomo, A. Covre, L. Sigalotti, A. Anichini, S. Coral, W.H. Fridman, C. Sautes-Fridman, Z. Trajanoski, M. Maio
Administrative, technical, or material support (i.e., reporting or organizing data, constructing databases): D. Giannarelli
Study supervision: A.M. Di Giacomo, A. Covre, M. Maio

Acknowledgments

We thank the Biomedical Sequencing Facility at CeMM for assistance with next-generation sequencing. We also thank Dr. Pier Giorgio Natali for his critical review of this article. Editorial assistance was provided by Jean Scott and was funded by the NIBIT Foundation. We thank the patients who participated in this study and their families.

The clinical trial and the translational studies received funding from the Associazione Italiana per la Ricerca sul Cancro (AIRC)—ID 15373 2014 (principal investigator M. Maio), from the FONDAZIONE AIRC under 5 per Mille 2018 – ID 21073 program (principal investigator M. Maio), and from an unrestricted grant from Astex Pharmaceuticals Inc. to the NIBIT Foundation. F. Finotello was supported by the Austrian Science Fund (FWF; project No. T 974-B30). Z. Trajanoski was supported by the Austrian Science Fund (FWF; project No. I3978 and I3291), Vienna Science and Technology Fund (Project LS16-025), and the European Research Council (AdG 786295).

The costs of publication of this article were defrayed in part by the payment of page charges. This article must therefore be hereby marked *advertisement* in accordance with 18 U.S.C. Section 1734 solely to indicate this fact.

Received April 23, 2019; revised July 23, 2019; accepted September 13, 2019; published first September 17, 2019.

References

1. Maio M, Covre A, Fratta E, Di Giacomo AM, Taverna P, Natali PG, et al. Molecular pathways: at the crossroads of cancer epigenetics and immunotherapy. Clin Cancer Res 2015;21:4040–7.
2. Sigalotti L, Fratta E, Coral S, Maio M. Epigenetic drugs as immunomodulators for combination therapies in solid tumors. Pharmacol Ther 2014; 142:339–50.
3. Sigalotti L, Fratta E, Coral S, Tanzarella S, Danielli R, Colizzi F, et al. Intratumor heterogeneity of cancer/testis antigens expression in human cutaneous melanoma is methylation-regulated and functionally reverted by 5-aza-2′-deoxycytidine. Cancer Res 2004;64:649167–71.
4. Fonsatti E, Nicolay HJ, Sigalotti L, Calabrò L, Pezzani L, Colizzi F, et al. Functional up-regulation of human leukocyte antigen class I antigens expression by 5-aza-2′-deoxycytidine in cutaneous melanoma: immunotherapeutic implications. Clin Cancer Res 2007;13:3333–8.
5. Coral S, Parisi G, Nicolay HJ, Colizzi F, Danielli R, Fratta E, et al. Immunomodulatory activity of SGI-110, a5-aza-2′-deoxycytidine-containing demethylating dinucleotide. Cancer Immunol Immunother 2013;62: 605–14.
6. Luo N, Nixon MJ, Gonzalez-Ericsson PI, Sanchez V, Opalenik SR, Li H, et al. DNA methyltransferase inhibition upregulates MHC-I to potentiate cytotoxic T lymphocyte responses in breast cancer. Nat Commun 2018;9:248.
7. Chiappinelli KB, Strissel PL, Desrichard A, Li H, Henke C, Akman B, et al. Inhibiting DNA methylation causes an interferon response in cancer via dsRNA including endogenous retroviruses. Cell 2015;162:974–86.
8. Fazio C, Covre A, Cutaia O, Lofiego MF, Tunici P, Chiarucci C, et al. Immunomodulatory properties of DNA hypomethylating agents: selecting the optimal epigenetic partner for cancer immunotherapy. Front Pharmacol 2018;9:1443.
9. Li X, Zhang Y, Chen M, Mei Q, Liu Y, Feng K, et al. Increased IFNg^{+}T cells are responsible for the clinical responses of low-dose DNA demethylating agent decitabine antitumor therapy. Clin Cancer Res 2017;23:6031–43.
10. Ghoneim HE, Fan Y, Moustaki A, Abdelsamed HA, Dash P, Dogra P, et al. De novo epigenetic programs inhibit PD-1 blockade-mediated T cell rejuvenation. Cell 2017;170:142–57.
11. Hodi FS, O'Day SJ, McDermott DF, Weber RW, Sosman JA, Haanen JB, et al. Improved survival with ipilimumab in patients with metastatic melanoma. N Engl J Med 2010;363:711–23.
12. Schadendorf D, Hodi FS, Robert C, Weber JS, Margolin K, Hamid O, et al. Pooled analysis of long-term survival data from phase II and phase III trials of ipilimumab in unresectable or metastatic melanoma. J Clin Oncol 2015; 33:1889–94.
13. Hodi FS, Chiarion-Sileni V, Gonzalez R, Grob JJ, Rutkowski P, Cowey CL, et al. Nivolumab plus ipilimumab or nivolumab alone versus ipilimumab alone in advanced melanoma (CheckMate 067): 4-year outcomes of a multicentre, randomised, phase 3 trial. Lancet Oncol 2018;19:1480–92.
14. Wei SC, Levine JH, Cogdill AP, Zhao Y, Anang NAS, Andrews MC, et al. Distinct cellular mechanisms underlie anti-CTLA-4 and anti-PD-1 checkpoint blockade. Cell 2017;170:1120–33.
15. Buchbinder EI, Desai A. CTLA-4 and PD-1 pathways: similarities, differences, and implications of their inhibition. Am J Clin Oncol 2016;39: 98–106.
16. Robert C, Schachter J, Long GV, Arance A, Grob JJ, Mortier L, et al. Pembrolizumab versus ipilimumab in advanced melanoma. N Engl J Med 2015;372:2521–32.
17. Rodig SJ, Gusenleitner D, Jackson DG, Gjini E, Giobbie-Hurder A, Jin C, et al. MHC proteins confer differential sensitivity to CTLA-4 and PD-1 blockade in untreated metastatic melanoma. Sci Transl Med 2018;10.
18. Covre A, Coral S, Nicolay H, Parisi G, Fazio C, Colizzi F, et al. Antitumor activity of epigenetic immunomodulation combined with CTLA-4 blockade in syngeneic mouse models. Oncoimmunology 2015;4:e1019978.
19. Covre A, Coral S, Di Giacomo AM, Taverna P, Azab M, Maio M. Epigenetics meets immune checkpoints. Semin Oncol 2015;42:506–13.

20. Roboz GJ, Kantarjian HM, Yee KWL, Kropf PL, O'Connell CL, Griffiths EA, et al. Dose, schedule, safety, and efficacy of guadecitabine in relapsed or refractory acute myeloid leukemia. Cancer. 2018;124:325–34.
21. Wolchok JD, Hoos A, O'Day S, Weber JS, Hamid O, Lebbé C, et al. Guidelines for the evaluation of immune therapy activity in solid tumors: immune-related response criteria. Clin Cancer Res 2009;15: 7412–20.
22. Federal Register 2013. Food and Drug Administration. Draft guidance for industry on bioanalytical method validation. Available from: https://www.federalregister.gov/documents/2013/09/13/2013–22309/draft-guidance-for-industry-on-bioanalytical-method-validation-availability.
23. Savoie N, Garofolo F, van Amsterdam P, Bansal S, Beaver C, Bedford P, et al. 2010 white paper on recent issues in regulated bioanalysis & global harmonization of bioanalytical guidance. Bioanalysis 2010;2: 1945–60.
24. Klughammer J, Datlinger P, Printz D, Sheffield NC, Farlik M, Hadler J, et al. Differential DNA methylation analysis without a reference genome. Cell Rep 2015;13:2621–33.
25. Akalin A, Kormaksson M, Li S, Garrett-Bakelman FE, Figueroa ME, Melnick A, et al. methylKit: a comprehensive R package for the analysis of genome-wide DNA methylation profiles. Genome Biol 2012;13:R87.
26. Barturen G, Rueda A, Oliver JL, Hackenberg M. MethylExtract: High-quality methylation maps and SNV calling from whole genome bisulfite sequencing data. Version 2. F1000Res 2013;2:217.
27. Wickham H. ggplot2 – Elegant graphics for data analysis. 2nd ed. In: Gentleman R, Hornik K, Parmigiani G, editors. New York: Springer; 2016.
28. Coral S, Sigalotti L, Gasparollo A, Cattarossi I, Visintin A, Cattelan A, et al. Prolonged upregulation of the expression of HLA class I antigens and costimulatory molecules on melanoma cells treated with 5-aza-2′-deoxycytidine (5-AZA-CdR). J Immunother 1999;22:16–24.
29. Prusty BK, Gulve N, Chowdhury SR, Schuster M, Strempel S, Descamps V, et al. HHV-6 encoded small non-coding RNAs define an intermediate and early stage in viral reactivation. NPJ Genom Med 2018;5:3–25
30. Bolger AM, Lohse M, Usadel B. Trimmomatic: a flexible trimmer for Illumina sequence data. Bioinformatics 2014;30:2114–20.
31. Dobin A, Davis CA, Schlesinger F, Drenkow J, Zaleski C, Jha S, et al. STAR: ultrafast universal RNA-seq aligner. Bioinformatics 2013;29:15–21.
32. Anders S, Pyl PT, Huber W. HTSeq–a Python framework to work with high-throughput sequencing data. Bioinformatics 2015;31:166–9.
33. Robinson MD, McCarthy DJ, Smyth GK. edgeR: a Bioconductor package for differential expression analysis of digital gene expression data. Bioinformatics 2010;26:139–40.
34. Robinson MD, Oshlack A. A scaling normalization method for differential expression analysis of RNA-seq data. Genome Biol 2010;11:R25.
35. Issa JJ, Roboz G, Rizzieri D, Jabbour E, Stock W, O'Connell C, et al. Safety and tolerability of guadecitabine (SGI-110) in patients with myelodysplastic syndrome and acute myeloid leukaemia: a multicentre, randomised, dose-escalation phase 1 study. Lancet Oncol 2015;16: 1099–110.
36. El-Khoueiry A, Mulcahy M, Bekaii-Saab T, Kim R, Denlinger CS, Goel R, et al. Single agent activity of the second-generation hypomethylating agent, SGI-110, in patients with hepatocellular carcinoma (HCC) after progression on sorafenib. ILCA Annual Conference, Paris, 4-6 September 2015 (abstract P-243).
37. Lee V, Wang J, Zahurak M, Gootjes E, Verheul HM, Parkinson R, et al. A phase I trial of a guadecitabine (SGI-110) and irinotecan in metastatic colorectal cancer patients previously exposed to irinotecan. Clin Cancer Res 2018;24:6160–7.
38. Matei D, Ghamande S, Roman L, Alvarez Secord A, Nemunaitis J, Markham MJ, et al. A phase I clinical trial of guadecitabine and carboplatin in platinum-resistant, recurrent ovarian cancer: clinical, pharmacokinetic, and pharmacodynamic analyses. Clin Cancer Res 2018;24:2285–93.
39. Zaretsky JM, Garcia-Diaz A, Shin DS, Escuin-Ordinas H, Hugo W, Hu-Lieskovan S, et al. Mutations associated with acquired resistance to PD-1 blockade in melanoma. N Engl J Med 2016;375:819–29.
40. Chang CC, Pirozzi G, Wen SH, Chung IH, Chiu BL, Errico S, et al. Multiple structural and epigenetic defects in the human leukocyte antigen class I antigen presentation pathway in a recurrent metastatic melanoma following immunotherapy. J Biol Chem 2015;290:26562–75.
41. Patel SJ, Sanjana NE, Kishton RJ, Eidizadeh A, Vodnala SK, Cam M, et al. Identification of essential genes for cancer immunotherapy. Nature 2017; 548:537–42.
42. Castro F, Cardoso AP, Gonçalves RM, Serre K, Oliveira MJ. Interferon-gamma at the crossroads of tumor immune surveillance or evasion. Front Immunol 2018;9:847.
43. Gao J, Shi LZ, Zhao H, Chen J, Xiong L, He Q, et al. Loss of IFN-γ pathway genes in tumor cells as a mechanism of resistance to anti-CTLA-4 therapy. Cell 2016;167:397–404.
44. Huang RR, Jalil J, Economou JS, Chmielowski B, Koya RC, Mok S, et al. CTLA4 blockade induces frequent tumor infiltration by activated lymphocytes regardless of clinical responses in humans. Clin Cancer Res 2011;17: 4101–9.
45. Sharma A, Subudhi SK, Blando J, Scutti J, Vence L, Wargo J, et al. Anti-CTLA-4 immunotherapy does not deplete FOXP3^{+} regulatory T cells (Tregs) in human cancers. Clin Cancer Res 2019;25:1233–8.